

# Molecular Structure, Mulliken charges, HOMO-LUMO, Electrostatic Potential and Nonlinear Optical Properties of Zwitterionic 6-methyl-2-oxo-3-[1-(ureidoiminio)ethyl]-2H-pyran-4-olate monohydrate molecule by HF and DFT methods

Nadia Benhalima<sup>1</sup>, Amel Djedouani<sup>2</sup>, Rachida Rahmani<sup>1</sup>, Abdelkader Chouaih<sup>1\*</sup>, Fodil Hamzaoui<sup>3</sup>, El Hadj Elandaloussi<sup>4</sup>

<sup>1</sup> Laboratory of Technology and Solid's Properties, Faculty of Sciences and Technology, Abdelhamid Ibn Badis University, BP 227 Mostaganem 27000, Algeria

<sup>2</sup> Ecole Normale Supérieure de Constantine, Constantine 25000, Algeria

<sup>3</sup> LPFM Academie de Montpellier, France

<sup>4</sup> Laboratoire de Valorisation des Matériaux, Université Abdelhamid Ibn Badis, B.P. 227, 27000 Mostaganem, Algeria

(Received December 07 2015, Accepted May 25 2016)

**Abstract.** In this work, we report a theoretical study on molecular structure, electrostatic potential and nonlinear optical properties of Zwitterionic 6-methyl-2-oxo-3-[1-(ureidoiminio)ethyl]-2H-pyran-4-olate monohydrate molecule (monomer and dimer). The molecular geometry in the ground state was investigated by ab initio and density functional method (B3LYP) with 6-31G(d) and 6-31+G(d,p) basis sets. The results show that the computed geometrical parameters are in good agreement with experimental values. The molecular electrostatic potential and HOMO-LUMO of the title molecule have been also calculated using the theoretical methods. The calculated HOMO and LUMO energies show that charge transfer occurs within the molecule. In order to investigate the nonlinear optical behavior, the electric dipole moment  $\mu$ , the polarizability  $\alpha$  and the hyperpolarizability  $\beta$  were computed. All  $\beta$  values that we report here are the magnitude of static hyperpolarizability. Theoretically predicted  $\beta$  values exhibit the higher nonlinear optical activity.

**Keywords:** theoretical calculation, charge transfer, atomic charges, molecular electrostatic potential, HOMO-LUMO

## 1 Introduction

Nonlinear optical (NLO) materials have been extensively studied for many years<sup>[2]</sup>. Materials with high NLO response are of great technological interest because of their potential applications in data storage, signal-processing, and telecommunication technologies<sup>[29]</sup>. In particular, organic molecules have received large attention due to the combination of molecular design flexibility, chemical tenability and choice of synthetic strategies<sup>[9]</sup>.

In the last two decades, organic molecules have been synthesized, some of them showing impressively high hyperpolarizabilities<sup>[19]</sup>. Theoretical investigations have been of great help in the achievement of these results; they gave the first hints about the possible high NLO responses of organic molecules with extended conjugated  $\pi$  systems<sup>[3]</sup>, and provided the guidelines for a rational design of such molecules<sup>[23]</sup>. The recent syntheses of zwitterionic molecules, some of them exhibiting extremely high NLO activity, have also been inspired by theoretical investigations<sup>[8]</sup>. Organic molecules with  $\pi$ -electron delocalization are currently of wide interest as NLO materials with potential applications in optical switches and other NLO devices<sup>[22]</sup>. Large

\* Corresponding author. E-mail address: achouaih@gmail.com

optical non-linearity could be seen in organic conjugated molecules incorporating an electron acceptor group at one moiety and a donor group at the opposite one<sup>[27]</sup>. For the prototypical push-pull molecule, the latter would exhibit an asymmetric polarization response to a symmetric electric field at intense field strengths since electron intensity is more easily displaced toward an acceptor substituent than toward a substituent donor<sup>[13]</sup>. Consequently, dipolar aromatic molecules possessing an electron donor group and an electron acceptor group contribute to large optical non-linearity arising from the intramolecular charge transfer between the two groups of opposite nature. It is also well known that the first and second hyperpolarizabilities in  $\pi$ -electron systems with donor-acceptor groups increase with increasing donor and acceptor strengths.

Despite the relevant role played by theory in the development of the field of NLO organic molecules, there are so far only few papers reported comparison between experimental and computed hyperpolarizability for large size NLO chromophores<sup>[11]</sup>. Zwitterionic compounds have received the interest of chemists and physicists due to their applications as nonlinear optical materials<sup>[18]</sup>. There are some reports concerning the formation of zwitterionic form in the crystal structure of ortho-hydroxy Schiff bases<sup>[28]</sup>.

The present work was assessed to the determination of the molecular structure, electrostatic potential and nonlinear optical properties of Zwitterionic 6-methyl-2-oxo-3-[1-(ureidoiminio)ethyl]-2H-pyran-4-olate monohydrate compound. A combined experimental and theoretical study was carried out and a detailed description of structural features of the studied molecule is reported. The ground state molecular structure was optimized and compared with experimental data obtained by X-ray analysis. In addition, various nonlinear optical properties such as electric dipole moment, molecular electrostatic potential, polarizability and hyperpolarizability were also addressed theoretically. The HOMO-LUMO energy gap has been computed and the NLO activity of the molecule was analyzed.

## 2 Computational details

The molecular geometries of the title compound were fully optimized at various theory levels using Gaussian 03 program<sup>[17]</sup> and Gauss-View molecular visualization program<sup>[1]</sup>. From X-ray crystal structure data<sup>[15]</sup>, Zwitterionic 6-methyl-2-oxo-3-[1-(ureidoiminio)ethyl]-2H-pyran-4-olate monohydrate compound crystallizes in the monoclinic space group P21/c with four molecules per unit cell ( $Z = 4$ ) and the following cell dimensions:  $a = 7.1731(4) \text{ \AA}$ ,  $b = 12.6590(10) \text{ \AA}$ ,  $c = 12.3698(3) \text{ \AA}$ .  $\beta = 104.603(6)^\circ$ . The data were collected at low temperature (173 K). The spatial coordinate positions of the title compound, as obtained from X-ray structural analysis, were used as initial coordinates for the theoretical calculations. For the title molecule, full geometry optimizations have been carried out at the Hartree-Fock (HF)<sup>[10]</sup> level using 6-31G(d) and 6-31+G(d,p) basis sets, by the Berny method<sup>[6, 16]</sup>. The effects of electron correlation on the geometry optimization are taken into account by Becke's three parameter hybrid exchange functions and Lee-Young-Parr correlation functional (B3LYP)<sup>[7, 30]</sup> level in the DFT method. The ab initio and DFT optimized geometries of the crystal structure of the investigated compound correspond to slightly non-planar conformation having 105° dihedral angle. The optimized structures were then used to calculate the electric dipole moments and hyperpolarizabilities of the title compound. Nonlinear optical calculations were performed at the both Hartree-Fock (HF) ab initio and DFT levels with 6-31G(d) and 6-31+G(d,p) basis sets. The 6-31G(d) basis set has been found to be more adequate for obtaining reliable trends in  $\beta$  values<sup>[14, 33]</sup>.

## 3 Results and discussion

### 3.1 Optimized geometry

The optimized bond lengths, bond and dihedral angles of the title compound calculated by B3LYP and HF methods using different basis sets are listed in Tab. 1, in accordance with atom numbering shown in Fig. 1. Our optimized structural parameters are now compared with the exact experimental X-ray data<sup>[15]</sup>. Tab. 1 shows that the most of bond lengths are found to be greater than experimental ones. For example, the calculated bond lengths (C1 N1, C1 N2, C2 N3, C4 C8, C4 C5, N2 N3) at B3LYP level are slightly larger than the corresponding

experimental values. This overestimation can be explained by the fact that the theoretical calculations belong to isolated molecule in gaseous phase and the experimental results belong to similar molecules in solid state. The  $C = O$  bond length namely  $C1\ O4$  ( $1.222\text{\AA}$ ),  $C5\ O1$  ( $1.215\text{\AA}$ ) and  $C8\ O3$  ( $1.258\text{\AA}$ ) calculated by means of B3LYP/6-31+G(d,p) method are most close to the measured ones. These values agree well with the data reported in the literature<sup>[4, 5]</sup>.

On the other hand, some computed bond angles deviate about  $1 - 2^\circ$  from the experimental data. The bond angles of  $O4\ C1\ N2$ ,  $C2\ N3\ N2$  and  $N3\ C2\ C3$  were measured to be  $121.02(17)$ ,  $124.75(15)$  and  $119.87(17)^\circ$ . The calculated values using B3LYP/6-31G(d) are of the order of  $123.52$ ,  $122.92$  and  $117.94^\circ$ , respectively.

According to the above comparisons, the biggest differences of bond lengths and bond angles mainly occur in the groups involved in the hydrogen bonding [i.e.,  $C1\ O4$ ,  $C8\ O3$  and  $N1\ C1\ N2$ ], which can also easily be understood taking into account the intermolecular hydrogen bond interactions occurring in the crystal.

When the X-ray structure of the title compound is compared with its optimized counterparts (see Fig. 2), slight conformational discrepancies are observed between them. The calculated value of dihedral angle ( $C1\ N2\ N3\ C2$ ) using both the B3LYP/6-31G(d) ( $108.4^\circ$ ) and HF/6-31G(d) ( $105.8^\circ$ ) methods is slightly different from the experimental one ( $0.00^\circ$ ). In the case of calculated dihedral angle, there is a good agreement between the B3LYP and HF methods. In spite of the differences observed, the calculated geometric parameters are in general in good agreement with the X-ray structure.

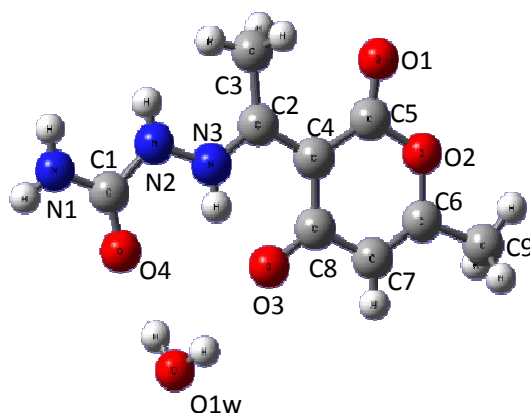


Fig. 1: Optimized structure with B3LYP/6-31G (d) level of the title molecule

### 3.2 Mulliken charge analysis

It is clear that the Mulliken<sup>[24]</sup> populations provide the simplest picture of the charge distribution. Knowledge of the charge density function can lead to some important properties of the molecule such as the charges on the different atoms, the molecular dipole moment and the electrostatic potential around the molecule. The Mulliken charges for the non-H atoms of the title compound were calculated at HF and B3LYP level with 6-31G(d) basis set in gas-phase. The atomic charges show that the  $N1$ ,  $N2$ ,  $N3$  and  $O1$ ,  $O1w$ ,  $O2$ ,  $O3$ ,  $O4$  atoms have bigger negative atomic charges in gas phase compared to carbon atoms. This behavior can be the result of intramolecular  $N - HO$  hydrogen bond and  $C8 = O3$  double bond features. The obtained results by both methods are summarized in Tab. 2.

### 3.3 Molecular electrostatic potential

Molecular electrostatic potential (MEP) is associated to the electronic density and has been used primarily for predicting sites and relative reactivities toward electrophilic attack in studies of biological recognition and

Table 1: Calculated geometrical parameters for the title molecule (Distance, Å; Angle, °)

Geometrical parameters	$X - ray^\alpha$	HF		DFT	
		6-31G(d)	6-31+G(d,p)	6-31G(d)	6-31+G(d,p)
C1-O4	1.227(2)	1.194	1.196	1.219	1.222
C1-N1	1.342(2)	1.36	1.358	1.374	1.37
C1-N2	1.375(2)	1.394	1.392	1.415	1.411
C2-N3	1.304(2)	1.325	1.324	1.341	1.34
C2-C4	1.452(2)	1.408	1.411	1.417	1.421
C2-C3	1.489(2)	1.506	1.504	1.502	1.5
C4-C8	1.423(2)	1.459	1.458	1.465	1.463
C4-C5	1.434(2)	1.457	1.457	1.457	1.457
C5-O1	1.217(2)	1.19	1.192	1.213	1.215
C5-O2	1.394(2)	1.365	1.364	1.408	1.406
C6-C7	1.325(2)	1.326	1.328	1.347	1.349
C6-O2	1.368(2)	1.343	1.343	1.357	1.359
C6-C9	1.490(3)	1.493	1.493	1.495	1.494
C7-C8	1.438(2)	1.459	1.458	1.452	1.45
C8-O3	1.282(2)	1.22	1.223	1.252	1.258
N2-N3	1.375(2)	1.374	1.374	1.391	1.39
O4-C1-N1	124.65(17)	124.12	123.88	124.31	124.05
O4-C1-N2	121.02(17)	123.31	123.09	123.52	123.06
N1-C1-N2	114.33(16)	112.56	113.02	112.16	112.89
N3-C2-C4	115.73(15)	119.51	119.14	118.93	118.06
N3-C2-C3	119.87(17)	117.66	117.91	117.94	118.45
C4-C2-C3	124.41(16)	122.82	122.94	123.13	123.49
C8-C4-C5	119.53(16)	119.18	119.04	119.8	119.64
C8-C4-C2	120.58(15)	121.67	121.74	121.53	121.43
C5-C4-C2	119.87(15)	119.13	119.22	118.66	118.92
O1-C5-O2	113.83(16)	115.3	115.38	114.6	114.79
O1-C5-C4	128.74(18)	127.54	127.39	128.4	128.2
O2-C5-C4	117.43(15)	117.16	117.22	117	117
C7-C6-O2	121.43(17)	122.33	122.19	122.15	121.93
C7-C6-C9	126.81(18)	126.39	126.46	126.2	126.35
O2-C6-C9	112.36(16)	111.28	111.35	111.65	111.72
C6-C7-C8	120.93(17)	120.77	120.65	121.27	121.13
O3-C8-C4	122.81(16)	124.17	123.93	123.53	123.11
O3-C8-C7	119.05(15)	119.44	119.46	119.76	119.83
C4-C8-C7	118.13(15)	116.38	116.61	116.71	117.06
C1-N2-N3	115.93(15)	116.13	116.45	115.6	116.26
C2-N3-N2	124.75(15)	123.57	123.64	122.92	123.15
C6-O2-C5	122.49(14)	124.17	124.29	123.07	123.23
C1-N2-N3-C2	0.00	105.8	104.55	108.41	105.62

hydrogen bonding interactions<sup>[25, 32]</sup>. Molecular electrostatic potential,  $V(r)$ , at a point  $r(x,y,z)$  is described as following:

$$V(r) = \sum_A \frac{Z_A}{|R_A - r|} - \int \frac{\rho(r') dr'}{r' - r}$$

$Z_A$  is the charge on nucleus A located at  $R_A$  and  $\rho(r)$  is the electron density. The electrostatic potential plots are shown in Fig. 2 ((a) monomer and (b) dimer). MEP was calculated at the B3LYP/6-31G(d) optimized geometry. The negative regions of MEP surface correspond to an attraction and are colored in red. While, the positive regions correspond to a repulsion and are colored in blue. The negative regions are related to electrophilic sites and the positive ones to nucleophilic sites. The MEP maps of the title molecule show that the negative regions were found around the oxygen atoms and that the positive potential sites are around the hydrogen atoms.

Table 2: Mulliken Charges (q) in the non-hydrogen atoms of the title molecule calculated with 6-31G(d) basis set

Atoms	q	
	HF	DFT
C1	-0.25	-0.223
C2	-0.243	-0.207
C3	-0.026	-0.035
C4	-0.038	-0.166
C5	-0.079	-0.077
C6	0.025	-0.146
C7	-0.098	0.102
C8	-0.026	-0.212
C9	-0.037	-0.078
N1	-0.037	-0.078
N2	-0.053	0.077
N3	0.134	-0.036
O1	0.207	0.221
O1w	0.213	0.243
O2	0.07	0.135
O3	0.06	0.133
O4	0.076	0.163

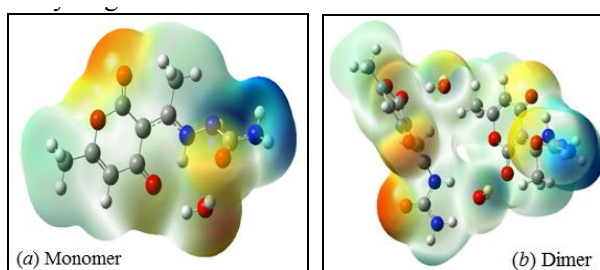


Fig. 2: Molecular electrostatic potential maps (a) and (b) calculated at B3LYP/6-31G(d) level

### 3.4 Homo-lumo calculation

The highest occupied molecular orbitals (HOMOs) and Lowest-lying unoccupied molecular orbitals (LUMO) are very useful for physicists and chemists because the energy difference between these orbitals (energy gap) represents the minimum energy required to promote an electron, and is therefore often the most-frequent and important energy transfer mechanism within a system. Further, the charge transport properties of the molecule<sup>[12]</sup> are determined by the difference of energy between HOMO and LUMO. The orbitals also provide important electron density information which can help determine which part of the molecule is most actively participating in an energy transfer event. The HOMO-LUMO energy gap of the molecule was calculated using HF/(6 - 31G(d) and 6 - 31 + G(d, p)) and B3LYP/(6 - 31G(d) and 6 - 31 + G(d, p)) level as presented in Tab. 3. The energy gap between HOMO and LUMO indicates molecular chemical stability. In addition, a lower HOMO-LUMO energy gap explains the fact that eventual charge transfer interaction is taking place within the molecule. The HOMO-LUMO plots are given in Fig. 3.

### 3.5 Hydrogen bonding and non linear optical properties

Hydrogen bonds are very important dipole interactions in stabilizing the structures. In amino acids having zwitterionic form, the NH<sub>2</sub> moiety is a good donor and the carboxylate or nitrate group is an excellent acceptor. In NLO crystals, hydrogen bonds linked with the adjacent molecules, where O-H...O hydrogen bonds are relatively stronger than N-H...O bonds<sup>[26]</sup>.

Fig. 4 shows the molecular packing diagram of the molecule where the hydrogen bond interactions N-H...O and O-H...O were observed. These interactions are responsible for the NLO effect in Zwitterionic

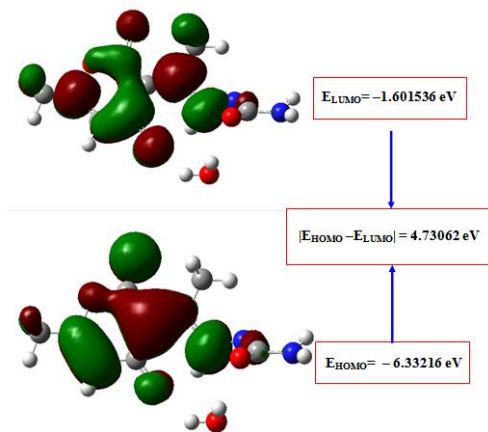


Fig. 3: The HOMO and LUMO plot of the title molecule

6-methyl-2-oxo-3-[1-(ureidoiminio)ethyl]-2H-pyran-4-olate monohydrate compound. The NLO effect may also be associated to the “push-pull” type structure. As expected, the best donors interact with the best acceptors leading to strong mentioned hydrogen bonds. These rigid hydrogen bonds link the symmetry-independent molecules into a dimer, which can be considered as the building block of the structure.

It is evident that the crystal structures are generated and stabilized by hydrogen bonds but more evidently that they also participate considerably to the increase of hyperpolarizability of hydrogen bonded molecular systems. For organic NLO materials, theoretical and experimental studies are performed in order to understand the microscopic origin of nonlinear behavior<sup>[20, 31]</sup>.

In this context, this study is extended to the determination of the electric dipole moment  $\mu$ , the isotropic polarizability  $\alpha$  and the first hyperpolarizability  $\beta_{tot}$  of the title compound (monomer and dimer). The dipole moment ( $\mu$ ), isotropic polarizability  $\beta_{tot}$ , first-order hyperpolarizability ( $\alpha$ ) tensor, can be obtained using the following equations:

$$\begin{aligned}\mu_0 &= (\mu_x^2 + \mu_y^2 + \mu_z^2)^{1/2} \\ \alpha &= \frac{1}{3}(\alpha_{xx} + \alpha_{yy} + \alpha_{zz}) \\ \beta_{tot} &= (\beta_x^2 + \beta_y^2 + \beta_z^2)^{1/2}.\end{aligned}$$

The whole equation for computing the magnitude of the first hyperpolarizability ( $\beta$ ) from Gaussian 03 output is given below:

$$\beta_{tot} = [(\beta_{xxx} + \beta_{yyy} + \beta_{zzz})^2 + (\beta_{yyy} + \beta_{yzz} + \beta_{yxx})^2] + (\beta_{zzz} + \beta_{zxx} + \beta_{zyy})^2$$

The first hyperpolarizability is a third rank tensor that can be depicted by a  $3 \times 3 \times 3$  matrices. The 27 components of the 3D matrix can be reduced to 10 components because of the Kleinman symmetry<sup>[21]</sup>. The Gaussian 03 output provides 10 components of this matrix as  $\beta_{xxx}$ ,  $\beta_{xxy}$ ,  $\beta_{xyy}$ ,  $\beta_{yyy}$ ,  $\beta_{xxz}$ ,  $\beta_{xyz}$ ,  $\beta_{yyz}$ ,  $\beta_{xzz}$ ,  $\beta_{yzz}$ ,  $\beta_{zzz}$  respectively.

The first hyperpolarizability tensors provided by Gaussian 03 are given in atomic units (a.u.), the computed values were converted into electrostatic units. ( $\alpha : 1a.u. = 0.1482 \times 10^{-24}esu$ ;  $\beta : 1a.u. = 8.6393 \times 10^{-33}esu$ ).

The dipole moment ( $\mu_0$ ), mean polarizability ( $\alpha$ ) and first hyperpolarizability ( $\beta$ ) for monomer and dimer are calculated at 6-31G(d) and 6-31+G(d,p) basis sets. Tab. 3 gives the HF and B3LYP results of the electronic dipole moment  $\mu_i$  ( $i = x, y, z$ ), polarizability  $\alpha_{ij}$  and the first hyperpolarizability  $\beta_{ijk}$  for Zwitterionic 6-methyl-2-oxo-3-[1-(ureidoiminio)ethyl]-2H-pyran-4-olate monohydrate compound (monomer and dimer). Theoretical calculation plays a significant role in understanding the structure-property relationship

which is able to help in designing novel NLO materials. It is well established that the higher values of dipole moment, molecular polarizability, and hyperpolarizability are very important for active NLO properties. The highest value of dipole moment obtained with B3LYP/Lan12dz is equal to 3.68 D for monomer and 12.32 D for dimer. The highest value of dipole moment is observed for component  $\mu_x$ . In this direction, this value is equal to 2.67 and 12.20 D for monomer and dimer respectively. The calculated polarizability ( $\alpha$ ), is equal to  $23.89 \times 10^{-24}$  esu and  $50.93 \times 10^{-24}$  esu for monomer and dimer respectively obtained with 6-31G+(d,p). As it can be seen in Tab. 3, the calculated polarizability  $\alpha_{ij}$  have non zero values and was dominated by the diagonal components. The first hyperpolarizability values  $\beta_{tot}$  of the title molecule obtained with B3LYP/Lan12dz are equal to  $3.553 \times 10^{-30}$  esu for monomer and  $14.568 \times 10^{-30}$  esu for dimer. The calculated results show that the title molecule might have microscopic nonlinear (NLO) behavior with non-zero values. The calculated first order hyperpolarizability of the title molecule has a low value of  $1.612 \times 10^{-30}$  esu obtained with HF method using 6-31+G(d,p) basis set and a high value of  $3.343 \times 10^{-30}$  esu obtained with DFT method using the same basis set. Thus, calculated low  $\beta$  total value for the title molecule ( $1.612 \times 10^{-30}$  esu) is found to be 8 times greater than the  $\beta$  total value of urea ( $0.1947 \times 10^{-30}$  esu), therefore, predicting that our molecule is a powerful candidate for NLO material.

From the cited above results, the molecule having the greatest  $\beta_{tot}$  value, corresponds to the low HOMO-LUMO energy gap. These results show that HOMO-LUMO gap have a substantial influence on the first hyperpolarizability. The high  $\beta$  value and low HOMO-LUMO energy gap show that the title molecule is highly NLO active material and it might be efficient for optoelectronic applications.

Consequently, we can finally infer from the above discussion of the contents of Tab. 3 that the introduction of electron correlation in the method applied for the analysis of the hyperpolarizability, such as DFT method, will probably predict more reasonable values as opposed to those converged upon use of the HF method.

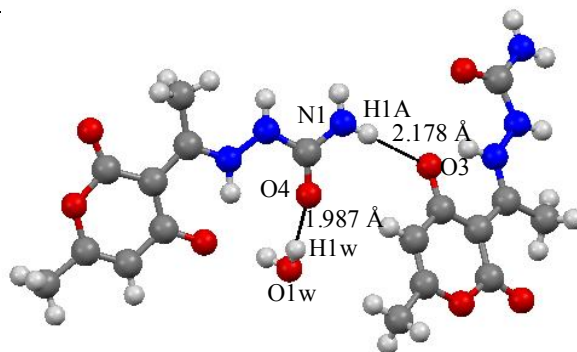


Fig. 4: N-H O and O-H O interactions calculated at B3LYP/6-31G (d) level

## 4 Conclusion

In this work we have calculated the geometric parameters and the nonlinear optical properties of the Zwitterionic 6-methyl-2-oxo-3-[1-(ureidoimino)ethyl]-2H-pyran-4-olate monohydrate molecule by using HF and B3LYP methods with 6-31G(d) and 6-31+G(d,p) basis sets. The optimized bond lengths and bond angles obtained with B3LYP level of calculation show the excellent agreement with the experimental values. The energy gap between HOMO and LUMO calculated using B3LYP is lower than the value calculated using HF level. The energy gap values indicate molecular chemical stability. Results show that the first hyperpolarizability  $\beta$  of Zwitterionic 6-methyl-2-oxo-3-[1-(ureidoimino)ethyl]-2H-pyran-4-olate monohydrate molecule is directly related to the HOMO-LUMO energy gap. Molecular electrostatic potential (MEP) was calculated at the B3LYP/6-31G (d) optimized geometry. The MEP map shows that the negative potential sites are on electronegative atoms as well as the positive potential sites are around the hydrogen atoms. These sites give

Table 3: The electric dipole moment  $\mu$  (D), the average polarizability  $\alpha(\times 10 - 24esu)$  and the first hyperpolarizability  $\beta(\times 10 - 30esu)$  of the title molecule

Parameters	HF				DFT			
	6 - 31G*		6 - 31 + G**		6 - 31G*		6 - 31 + G*	
	Monomer	Dimer	Monomer	Dimer	Monomer	Dimer	Monomer	Dimer
$\mu_x$	-2.43	10.7	-2.49	10.23	2.43	7.52	-2.2	-9.54
$\mu_y$	-1.01	1.16	-0.85	1.52	1.49	3.92	-1.75	-0.89
$\mu_z$	-1.46	2.88	-1.76	1.31	-1.12	-0.02	-1.68	1.41
$\mu$	3.01	11.14	3.16	10.43	3.06	8.48	3.28	9.68
$\alpha_{xx}$	117.91	340.7	133.68	372.29	137.27	406.38	158.59	450.83
$\alpha_{xy}$	7.59	24.42	5.71	22.45	13.2	42.35	11.7	39.31
$\alpha_{yy}$	84.7	294.76	102.7	324.47	90.71	340.37	113.99	382.3
$\alpha_{xz}$	-10.03	4.7	-7.72	3.38	-18.2	3.19	-15.3	1.92
$\alpha_{yz}$	-30.44	-19.92	-28.71	-18.25	-38.04	-20.45	-37.12	-20.12
$\alpha_{zz}$	158.67	143.03	174.42	182.59	188.35	150.33	211.03	197.92
$\alpha(a.u)$	120.43	259.5	136.93	293.12	138.78	299.03	161.2	343.68
$\alpha(esu)$	17.85	38.46	20.29	43.44	20.57	44.32	23.89	50.93
$\beta_{xxx}$	-185.58	-328.15	-227.43	-380.87	-243.11	-971.9	-305.38	-1017.81
$\beta_{xxy}$	8.23	348.55	9.21	409.36	1.26	21.76	1.99	125.01
$\beta_{xyy}$	74.72	76.27	40.78	96.08	76.95	-295.54	43.75	-252.36
$\beta_{yyy}$	11.22	-362.16	18.73	-402.67	27.48	-782.81	43.7	-812.12
$\beta_{xxz}$	-5.92	-129.39	-16.07	-91.6	2.41	-111.63	-19.18	-74.57
$\beta_{xyz}$	-87.03	-19.42	-108.2	-26.28	-87.27	-82.28	-120.81	-75.47
$\beta_{yyz}$	-16.29	39.5	-18.41	64.5	-33.89	-67.97	-48.9	-12.34
$\beta_{xzz}$	262.48	-3.82	279.76	-2.33	277.38	-71.4	323.42	-55.41
$\beta_{yzz}$	28.38	-16.31	33.64	-13.91	59.7	-67.12	76.06	-51.41
$\beta_{zzz}$	-113.47	22.96	-115.11	32.39	-260.4	29.08	-294.05	47.83
$\beta(a.u)$	209.01	266	186.65	287.26	324.63	1581.46	387.01	1517.93
$\beta(esu)$	1.806	2.298	1.612	2.482	2.804	13.663	3.343	13.114
HOMO	-0.3331	-0.326	-0.3392	-0.331	-0.2328	-0.2043	-0.2475	-0.2239
LUMO	0.0922	0.0826	0.0532	0.0438	-0.0589	-0.0749	-0.075	-0.0819
Gap (Hartrees)	0.4253	0.4086	0.3924	0.3748	0.1739	0.1294	0.1725	0.142
Gap (ev)	11.5731	11.1187	10.6778	10.1989	4.7321	3.5212	4.694	3.864

information about the region from where the compound can have intramolecular interactions. This study reveals that Zwitterionic 6-methyl-2-oxo-3-[1-(ureidoiminio)ethyl]-2H-pyran-4-olate monohydrate molecule has a large first static hyperpolarizabilities and may have potential applications in the development of NLO materials.

## References

- [1] A. H. A. Frisch, A.B. Neilson. Gauss view 4, gaussian, inc., wallingford ct 06492 usa, 2009.
- [2] P. Agarwal, N. Choudhary. Density functional theory studies on the structure, spectra (ft-ir, ft-raman, and uv) and first order molecular hyperpolarizability of 2-hydroxy-3-methoxy-n-(2-chloro-benzyl)-benzaldehyde-imine: Comparison to experimental data. *Vibrational Spectroscopy*, 2013, **64**((2013)): 134–147.
- [3] G. P. Agrawal, C. Flytzanis. Delocalization and superalternation effects in the nonlinear susceptibilities of one-dimensional systems. *Chemical Physics Letters*, 1976, **44**(2): 366–370.
- [4] M. I. Attia, N. R. El-Brollosy. Synthesis, single crystal x-ray structure, and antimicrobial activity of 6-(1,3-benzodioxol-5-ylmethyl)-5-ethyl-2-[2-(morpholin-4-yl)ethyl]sulfanylpyrimidin-4(3h)-one. *Journal of Chemistry*, 2015, **2014**(4): 1–8.
- [5] M. I. Attia, H. A. Ghabbour et al Synthesis and single crystal x-ray structure of new (2e)-2-[3-(1h-imidazol-1-yl)-1-phenylpropylidene]-n-phenylhydrazinecarboxamide. *Journal of Chemistry*, 2013, **2013**.
- [6] R. F. W. Bader. Atoms in molecules: A quantum theory. 1994, **360**(1-3).
- [7] A. D. Becke. Density-functional thermochemistry. v. systematic optimization of exchange-correlation functionals. *The Journal of chemical physics*, 1997, **107**(20): 8554–8560.



- [8] A. Capobianco, A. Esposito, T. Caruso. Tuning wavefunction mixing in pushpull molecules: From neutral to zwitterionic compounds. *European Journal of Organic Chemistry*, 2012, **2012**(15): 2980–2989.
- [9] R. Centore, A. Concilio, F. Borbone. Quadratic nonlinear optical and preliminary piezoelectric investigation of crosslinked samples obtained from a liquid chromophore. *Journal of Polymer Science Part B Polymer Physics*, 2012, **50**(9): 650–655.
- [10] H. D. Cohen, C. C. J. Roothaan. Electric dipole polarizability of atoms by the hartree-fock method. *Journal of Chemical Physics*, 1965, **43**(10): S34–S39.
- [11] L. R. Dalton, S. J. Benight. Systematic nanoengineering of soft matter organic electro-optic materials. *Chemistry of Materials*, 2011, **23**(3): 430–445.
- [12] W. B. Davis, W. A. Svec, M. A. Ratner. Molecular-wire behaviour in p -phenylenevinylene oligomers. *Nature*, 1998, **396**(6706): 60–63.
- [13] B. L. Davydov, L. D. Derkacheva, V. V. Dunina. Connection between charge transfer and laser second harmonic generation. *Zhetf Pisma Redaktsiiu*, 1970, **12**(1): 24.
- [14] C. Dehu, F. Meyers, et al Solvent effects on the second-order nonlinear optical response of pi.-conjugated molecules: A combined evaluation through self-consistent reaction field calculations and hyper-rayleigh scattering measurements. *Journal of the American Chemical Society*, 1995, **117**(40): 10127–10128.
- [15] A. Djedouani, S. Boufas. Djedouani, a., boufas, s., allain, m., bouet, g., khan, m.: Zwitterionic 6-methyl-2-oxo-3-[1-(ureidoiminio)ethyl]-2h-pyran-4-olate monohydrate. *Acta Crystallogr Sect E Struct Rep Online*, 2008, **64**(Pt 9): 1785–1793.
- [16] R. Fletcher, M. J. D. Powell. A rapidly convergent descent method for minimization. *Computer Journal*, 1963, **6**(6): 163–168.
- [17] M. Frisch, G. Trucks, et al J. Cheeseman, et al. Gaussian 03, revision b. 04. gaussian, inc., pittsburgh, 2003.
- [18] M. P. Hill, E. C. Carroll et al Rapid photodynamics of vitamin b6 coenzyme pyridoxal 5'-phosphate and its schiff bases in solution. *Journal of Physical Chemistry B*, 2008, **112**(18): 5867.
- [19] H. Kang, A. Facchetti, H. Jiang. Ultralarge hyperpolarizability twisted pi-electron system electro-optic chromophores: synthesis, solid-state and solution-phase structural characteristics, electronic structures, linear and non-linear optical properties, and computational studies. *Journal of the American Chemical Society*, 2007, **129**(11): 3267–86.
- [20] P. Kerkoc, M. Zgonik, K. Sutter. 4-(n,n-dimethylamino)-3-acetamidonitrobenzene single crystals for nonlinear-optical applications. *Journal of the Optical Society of America B*, 1990, **7**(3): 313–319.
- [21] D. A. Kleinman. Nonlinear dielectric polarization in optical media. *Physical Review*, 1962, **126**(6): 1977–1979.
- [22] M. Lanata, C. Bertarelli et al Molecules with quinoid ground state: a new class of large molecular optical nonlinearities. *Synthetic Metals*, 2003, **138**(1-2): 357–362.
- [23] S. R. Marder, B. Kippelen, et al Design and synthesis of chromophores and polymers for electro-optic and photorefractive applications. *Nature*, 1997, **388**(6645): 845.
- [24] R. S. Mulliken. Electronic population analysis on lcao–mo molecular wave functions. i. *The Journal of Chemical Physics*, 1955, **23**(10): 1833–1840.
- [25] J. S. Murray, K. D. Sen. *Molecular electrostatic potentials : concepts and applications*. Elsevier, 1996.
- [26] H. S. Nalwa, M. Hanack. Third-order nonlinear optical properties of porphyrazine, phthalocyanine and naphthalocyanine germanium derivatives: Demonstrating the effect of -conjugation length on third-order optical nonlinearity of two-dimensional molecules. *Chemical physics*, 1999, **245**(1): 17–26.
- [27] H. S. e. a. Nalwa. *Nonlinear Optics of Organic Molecules and Polymers*. 1997.
- [28] A. Ozek, C. Albayrak. Three (e)-2-[(bromophenyl)iminomethyl]-4-methoxyphenols. *Acta Crystallographica Section C-crystal Structure Communications*, 2007, **63**(3): 177–180.
- [29] A. Petrosyan. Salts of l-histidine as nonlinear optical materials: a review. *J Cryst Phys Chem*, 2010, **1**(1): 33–56.
- [30] G. Rauhut, P. Pulay. Transferable scaling factors for density functional derived vibrational force fields. *J.phys.chem*, 1995, **99**(10): 3093–3100.
- [31] D. Sajan, H. J. Ravindra, N. Misra. Intramolecular charge transfer and hydrogen bonding interactions of nonlinear optical material n -benzoyl glycine: Vibrational spectral study. *Vibrational Spectroscopy*, 2010, **54**(1): 72–80.
- [32] E. Scrocco, J. Tomasi. Electronic molecular structure, reactivity and intermolecular forces: An euristic interpretation by means of electrostatic molecular potentials. *Advances in Quantum Chemistry*, 1978, **11**: 115–193.
- [33] K. S. Thanthiriwatte, K. M. N. D. Silva. Non-linear optical properties of novel fluorenyl derivatives: ab initio quantum chemical calculations. *Journal of Molecular Structure Theochem*, 2002, **617**(1-3): 169–175.